AUTOPHAGY
2023, VOL. 19, NO. 7, 2094–2110
https://doi.org/10.1080/15548627.2023.2172873

Taylor & Francis
Taylor & Francis Group

RESEARCH PAPER

PRKN/parkin-mediated mitophagy is induced by the probiotics *Saccharomyces boulardii* and *Lactococcus lactis*

Peter John Hawrysh[a], Jinghua Gao[a], Stephanie Tan[a], Amy Oh[a], Justin Nodwell[a], Thomas A. Tompkins[b], and G. Angus McQuibban[a]

[a]Department of Biochemistry, University of Toronto, Toronto, ON, Canada; [b]Lallemand Bio Ingredients, Montreal, QC, Canada

ABSTRACT

Mitochondrial impairment is a hallmark feature of neurodegenerative disorders, such as Parkinson disease, and PRKN/parkin-mediated mitophagy serves to remove unhealthy mitochondria from cells. Notably, probiotics are used to alleviate several symptoms of Parkinson disease including impaired locomotion and neurodegeneration in preclinical studies and constipation in clinical trials. There is some evidence to suggest that probiotics can modulate mitochondrial quality control pathways. In this study, we screened 49 probiotic strains and tested distinct stages of mitophagy to determine whether probiotic treatment could upregulate mitophagy in cells undergoing mitochondrial stress. We found two probiotics, *Saccharomyces boulardii* and *Lactococcus lactis*, that upregulated mitochondrial PRKN recruitment, phospho-ubiquitination, and MFN degradation in our cellular assays. Administration of these strains to *Drosophila* that were exposed to paraquat, a mitochondrial toxin, resulted in improved longevity and motor function. Further, we directly observed increased lysosomal degradation of dysfunctional mitochondria in the treated *Drosophila* brains. These effects were replicated *in vitro* and *in vivo* with supra-physiological concentrations of exogenous soluble factors that are released by probiotics in cultures grown under laboratory conditions. We identified methyl-isoquinoline-6-carboxylate as one candidate molecule, which upregulates mitochondrial PRKN recruitment, phospho-ubiquitination, MFN degradation, and lysosomal degradation of damaged mitochondria. Addition of methyl-isoquinoline-6-carboxylate to the fly food restored motor function to paraquat-treated *Drosophila*. These data suggest a novel mechanism that is facilitated by probiotics to stimulate mitophagy through a PRKN-dependent pathway, which could explain the potential therapeutic benefit of probiotic administration to patients with Parkinson disease.

ARTICLE HISTORY
Received 24 May 2022
Revised 19 January 2023
Accepted 20 January 2023

KEYWORDS
Drosophila; melanoxadin; methyl-isoquinoline -6-carboxylate; mitochondria; PRKN/parkin; parkinson disease; picolinic acid

Introduction

Parkinson disease (PD) is the second most common neurodegenerative disorder, affecting 2–3% of individuals over 65 years of age [1]. It is a complex motor disorder that is characterized by the progressive loss of dopaminergic neurons in the substantia nigra pars compacta, leading to tremors, rigidity, bradykinesia, and loss of fine motor control. Given that there is no cure for PD following its diagnosis, there is an increased importance in understanding its etiology and developing prophylactic measures that can delay or even prevent the onset of symptoms. While most PD cases are idiopathic in origin, 15% of cases are familial in origin [2] and many of the autosomal recessive genes implicated in hereditary PD encode for proteins either directly [3,4] or indirectly [5–10] involved in maintaining the integrity of the mitochondrial network through the selective macroautophagy/autophagy of dysfunctional mitochondria, termed mitophagy.

The most described mitophagy pathway is controlled by PINK1 (PTEN induced kinase 1) and the E3 ubiquitin ligase PRKN/parkin/PARK2. In healthy mitochondria, PINK1 is rapidly cleaved for proteasomal degradation, however mitochondrial depolarization disrupts this process and results in accumulation of PINK1 on the outer mitochondrial membrane (OMM) [11]. Accumulated PINK1 phosphorylates both basal ubiquitin on OMM proteins and PRKN's ubiquitin-like domain at Ser65, which activates and recruits PRKN to the OMM to conjugate additional ubiquitin onto OMM proteins. The PINK1-PRKN system also rapidly ubiquitinates the fusion proteins MFN1 (mitofusin 1) and MFN2 and marks them for degradation, which facilitates the removal of damaged mitochondria from the healthy mitochondrial pool [12]. Following its addition, ubiquitin is phosphorylated by PINK1 which generates a positive feedback loop that ultimately signals for autophagosome recognition and lysosomal degradation [13]. Loss of function mutations in Pink1 and park in *Drosophila* lead to fragmented mitochondrial cristae, increased sensitivity to oxidative stress, and dopaminergic neuronal degeneration accompanied by locomotive defects [14,15]. PINK1 and PRKN mutations also impair ubiquitination and degradation of MFN1 and MFN2 following mitochondrial depolarization, impeding mitochondrial fission [16]. Given that mutations in PINK1 and PRKN are associated with early-onset PD in humans [3,4] and are also observed in cases of sporadic PD [17], it suggests that the accumulation of dysfunction mitochondria leads to disease onset and upregulation of mitophagy may be a solution to delay or prevent disease progression.

CONTACT G. Angus McQuibban angus.mcquibban@utoronto.ca Department of Biochemistry, University of Toronto, Toronto, ON, Canada M5G 1M1
Supplemental data for this article can be accessed online at https://doi.org/10.1080/15548627.2023.2172873

While *pink1* and *prkn* knockout mice exhibit little to no impairments to motor function or dopaminergic neuron viability [18]; strikingly, intestinal infection with Gram-negative bacteria induces motor impairment and a loss of dopaminergic neuron projections in the striatum of *pink1* knockout mice, which are phenotypes strongly associated with PD [19]. The gut has been proposed to be a point of origin for PD pathology, as PD subjects exhibited an increased intestinal permeability to bacterial agents [20] and elevated levels of Lewy bodies in enteric nerve plexuses [21]. Intestinal injection of alpha-synuclein preformed fibrils in rats led to progressive PD-like pathology and this is prevented following removal of the vagus nerve, suggesting a gut-brain axis of communication that is involved in neurological decline [22]. Intestinal inflammation is linked to the composition of the gut microbiota and a common symptom of PD patients is gut dysbiosis [23,24], which suggests that healing the gut microbiome with probiotics could be a solution to improve disorder outcomes. Probiotic supplementation has been used to improve constipation and metabolic profiles in PD patients [25,26] and facilitates the recovery of mitochondrial function while alleviating motor function deterioration in various rodent PD models [27,28]. Taken together, these data suggest a mechanistic link between probiotics and the alleviation of neurodegenerative disorders. We therefore sought to determine whether probiotics ameliorate neurological mitochondrial disorders by upregulating mitophagy pathways and facilitating the removal of damaged mitochondria.

In this study, we conducted a screen of 49 probiotic strains and formulations using several cellular assays at critical steps in the mitophagy pathway [29] to determine whether probiotics that modulate mitophagy can be identified. Overall, this work identified *Saccharomyces boulardii* (CNCM-I-1079) and *Lactococcus lactis* (R1058), as two strains that promote mitophagy in models of mitochondrial dysfunction. Further, one metabolite that is secreted by these probiotics, methyisoquinoline-6-carboxylate, was discovered to promote mitophagy induction in models of mitochondrial stress through a PRKN-dependent process.

Results

A mitophagy screen reveals that probiotics increase mitochondrial PRKN recruitment following CCCP-induced mitochondrial dysfunction

To investigate whether probiotics modulate mitophagy, we performed a screen using a cell-based assay that tests for factors that modulate mitochondrial PRKN recruitment, an early indicator of mitophagy induction. This assay utilizes a HEK293 cell line that stably expresses GFP-tagged PRKN and has been established as an effective tool to screen for small molecules that promote mitophagy via mitochondrial PRKN recruitment [29]. We utilized Lallemand Health Solutions' commercial library of probiotics for this screen by co-culturing GFP-PRKN HEK293 cells with candidate probiotics and screening for probiotic formulations that increased the proportion of cells with elevated levels of mitochondrially-localized PRKN following mitochondrial stress via exposure to the protonophore, carbonyl cyanide m-chlorophenyl hydrazone (CCCP).

Using supervised machine-learning analysis, we found that the proportion of GFP-PRKN HEK293 cells exhibiting mitochondrially localized PRKN following a 2 h incubation period with CCCP alone was 22.1 ± 4.2% (Figure 1A, E), while incubation with a DMSO vehicle yielded 1.5 ± 1.0%. We next tested whether a 3 h pre-incubation with probiotic cultures at a multiplicity of infection (MOI) of 100:1 resulted in a modulation of mitochondrial PRKN recruitment. From the 49 probiotic formulations that were tested (Figure 1A), we found that 5 probiotics (Figure 1B) resulted in a significant elevation in mitochondrial PRKN recruitment: *Bacillus subtilis* (R0179), *Enterococcus faecium* (R0026), *Saccharomyces boulardii* (CNCM-I-1079), *Lactococcus lactis* (R1058), and IBacilluS+ blend (90% R0026 and 10% R0179). These strains, with the exception of R0179, also resulted in a significant elevation of mitochondrial PRKN recruitment at a MOI of 50:1 but not 10:1 (Figure 1C, G). Pre-incubation of GFP-PRKN HEK293 cells with *Lactobacillus casei* (HA108, strain #32) also induced an observable increase in PRKN recruitment following CCCP treatment (Figure 1A), but this was not statistically significant relative to the CCCP baseline of the specific experiments that tested this strain ($p = 0.1879$). GFP-PRKN cells that were pre-incubated with probiotics and treated with a DMSO vehicle instead of CCCP did not undergo PRKN recruitment (Figure 1C, D, F), indicating that probiotic co-cultures do not induce mitochondrial PRKN recruitment in the absence of CCCP-mediated mitochondrial stress.

Probiotics elevate mitochondrial phospho-ubiquitination and MFN2 degradation following CCCP-induced mitochondrial dysfunction

We next sought out to determine whether the top probiotic candidates from the PRKN recruitment screen also regulated later stages of mitophagy, specifically mitochondrial phospho-ubiquitination and MFN2 degradation. GFP- PRKN HEK293 cells that were co-cultured with probiotics for 3 h and treated with CCCP for 2 h were immunohistochemically stained for Ser65-phosphorylated Ub (ubiquitin; p-Ub) and analyzed for PRKN and p-Ub mitochondrial co-localization. In the absence of probiotic pre-treatment, CCCP exposure led to 6.2 ± 1.7% ($n = 3$) of cells expressing colocalized PRKN and p-Ub fluorescence, while a DMSO vehicle alone led to an absence of cells with PRKN and p-Ub colocalization ($n = 3$). Of the top 5 probiotic samples that were identified in the GFP-PRKN screen, there were 4 probiotics that resulted in a significant elevation in mitochondrial phospho-ubiquitination following CCCP treatment: R0026 at MOIs of 100:1 and 50:1, CNCM-I-1079 at MOIs of 100:1 and 50:1, R1058 at MOIs of 100:1 and 50:1, and the IBacilluS+ blend at MOIs of 100:1, 50:1, and 10:1. There was no significant difference following a pre-incubation with R0179 at any MOI before incubation with CCCP (Figure 2A,B). To verify that treatment with probiotics alone does not increase phospho-ubiquitination, cells were co-cultured with probiotics and treated with a DMSO vehicle, which led to no increase in p-Ub expression with any of the candidate probiotic strains (Figure 2A,B). To verify that the

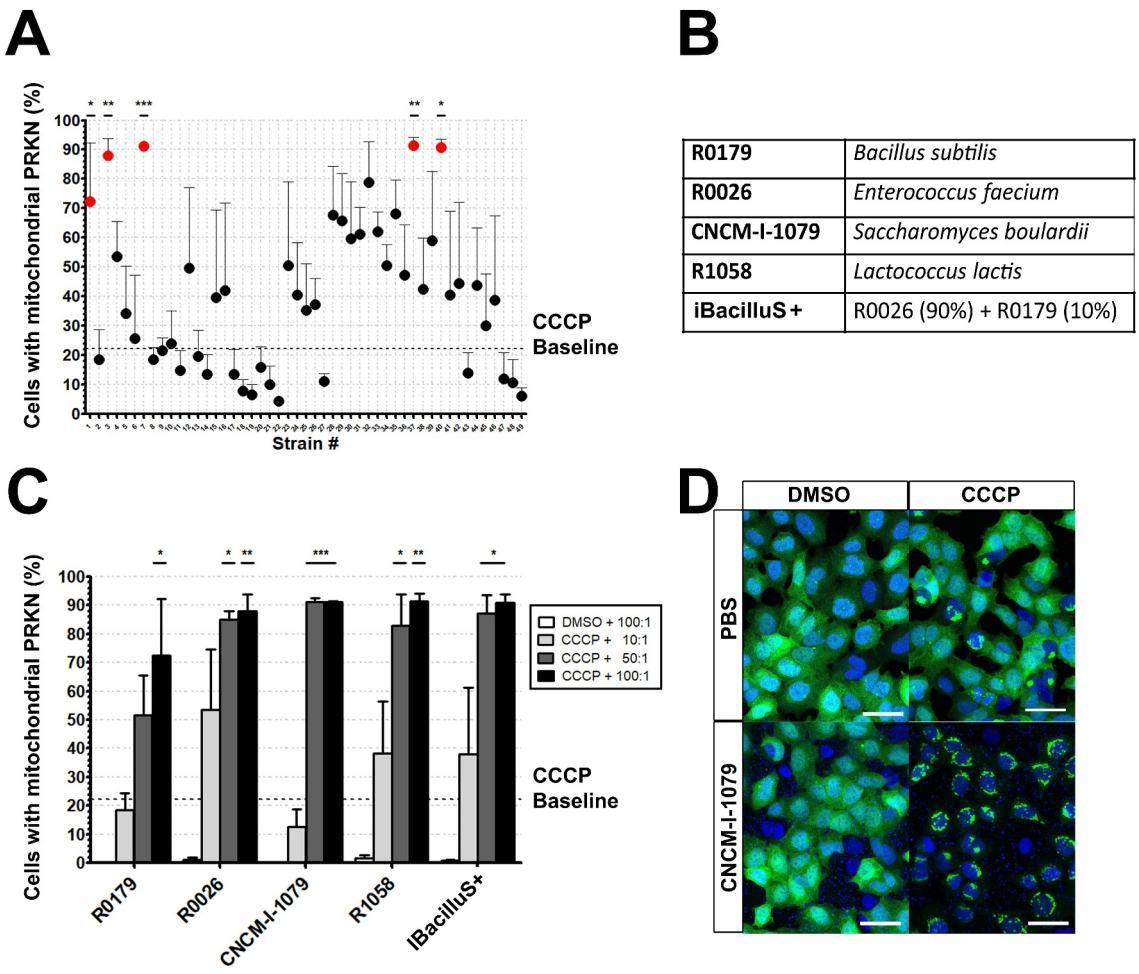

Figure 1. Probiotic co-cultures increased PRKN recruitment to CCCP-stressed mitochondria. (A), mitochondrial PRKN recruitment in HEK293 cells in response to pre-incubation with probiotics (MOI = 100:1, 3 h, n = 3) and subsequent CCCP stress (6.0 μM, 2 h). The dotted line represents the average baseline PRKN recruitment following CCCP stress in the absence of probiotic pre-incubation across all experiments. Strain numbers correspond to individual strains that were blind-tested and are defined in Table S1. The top four strains and one blend (B and C) were tested at MOIs of 100:1, 50:1, and 10:1 (100, 50, or 10 colony forming units added per HEK293 cell) in the presence of either CCCP or a DMSO vehicle. All data are represented as the mean ± S.E.M. (n = 3 for all strains). An asterisk indicates a statistically significant increase from baseline in the absence of probiotic pre-incubation (where * represents $p < 0.05$, ** represents $p < 0.01$, and *** represents $p < 0.0001$). Sample images represent cells that were treated with DMSO and a PBS blank (D), CCCP and a PBS blank (E), DMSO and 100:1 CNCM-I-1079 (F), and CCCP and 100:1 CNCM-I-1079 (G). Scale bars: 50 μm.

elevated phospho-ubiquitination response is specific to the top candidates from the GFP-PRKN screen, we co-cultured GFP-PRKN HEK293 cells with *Lactobacillus delbrueckii bulgaricus* (R0440), a probiotic strain that did not promote any significant mitochondrial PRKN recruitment in the screen. Following a pre-incubation with R0440, there was no change in p-Ub expression at any MOI (Figure 2A).

To test whether probiotics are also modulating the stability of proteins involved in mitochondrial fusion during mitochondrial dysfunction, we analyzed MFN2 levels following CCCP-mediated mitochondrial stress in the presence or absence of a probiotic pre-incubation period. MFN1 and MFN2 are large OMM GTPases that mediate mitochondrial fusion and are rapidly ubiquitinated by PRKN following the induction of mitophagy to prevent refusion of damaged mitochondria with the healthy pool [30,31]. MFN2 is necessary for mediating PRKN recruitment to mitochondria following PINK1 phosphorylation by serving as a PRKN binding target through p-Ub moieties and is one of the first mitochondrial outer membrane proteins to be degraded [32,33]. Given its rapid degradation, MFN2 was used in this study as a marker for early mitophagy induction. Incubation of GFP-PRKN HEK293 cells with 6.5 μM CCCP for 90 min reduced MFN2 levels to 0.80 ± 0.18 (n = 3) when normalized to MFN2 levels in cells treated with DMSO alone (Figure 2C). Cells were pretreated with either the top probiotic candidates from the GFP-PRKN screen, or the negative control R0440, followed by CCCP to determine whether probiotics potentiate CCCP-mediated MFN2 degradation. Of the 5 probiotic candidates, CNCM-I-1079 and R1058 both caused a significant reduction in MFN2 levels following CCCP stress at MOIs of 100:1 and 50:1 when compared to cells treated with CCCP alone. R0179 caused a significant reduction in MFN2 levels following CCCP stress at MOIs of 10:1. R0026, IBacillus+ blend, and the negative control R0440 did not significantly alter MFN2 protein levels at any MOI following CCCP stress (Figure 2C-D, FigureS1A-E). These data suggest that in addition to promoting mitochondrial PRKN recruitment and phospho-ubiquitination as a means for selective mitochondrial degradation, CNCM-I-1079 and R1058 also facilitate MFN2

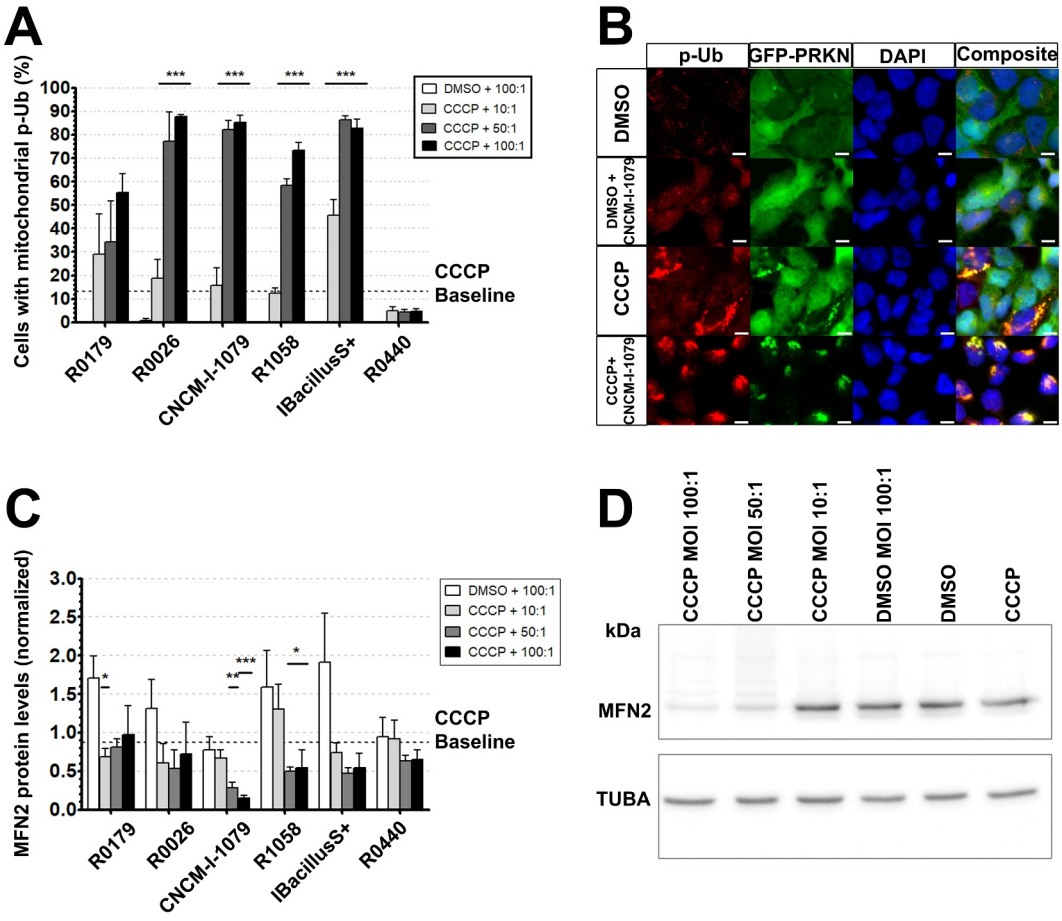

Figure 2. Probiotic co-cultures elevated CCCP-mediated mitochondrial poly-ubiquitination and MFN2 degradation. (A), phospho-ubiquitin (p-Ub) expression in GFP-PRKN HEK293 cells that were co-cultured with 6 probiotic strains in three different MOIs and treated with either CCCP (6.5 μM, 2 h) or a DMSO vehicle. The dotted line represents the average p-Ub expression following CCCP stress in the absence of probiotic pre-incubation. (B), sample images are shown for cells treated with CNCM-I-1079 (MOI = 100:1) and stained for DAPI (blue), GFP-PRKN (green), and anti-Ser65-pUb (red). Scale bars: 50 μm. (C), MFN2 expression in GFP-PRKN HEK293 cells that were co-cultured with 6 probiotic strains and treated with either CCCP (6.5 μM, 1.5 h) or a DMSO vehicle. Data are expressed as the ratio of MFN2:TUBA band density, divided by the MFN2:TUBA ratio band density obtained from cells exposed to DMSO only. The dotted line represents average MFN2 protein levels following CCCP stress in the absence of probiotic pre-incubation. (D), sample western blot for cells exposed to either a PBS vehicle or CNCM-I-1079, and either DMSO or CCCP. All data are mean ± SEM (n = 3 for all strains). Asterisks represent data sets that are significantly different from baseline (* represents $p < 0.05$, ** represents $p < 0.01$, and *** represents $p < 0.001$).

degradation to reduce integration of dysfunctional mitochondria into the healthy mitochondrial network.

Probiotics lead to elevated lysosomal degradation of neuronal mitochondria in vivo, improved climbing ability, and extended longevity in Drosophila *models of mitochondrial dysfunction*

To gain further insight into the role of probiotics on mitophagy, we next tested the effect that probiotics have on autophagosome formation by assaying MAP1LC3/LC3 (microtubule associated protein 1 light chain 3) levels. Once synthesized, LC3 precursor protein is converted into the cytosolic protein LC3-I. Upon induction of autophagy, LC3-I is converted into LC3-II by ubiquitin-like conjugation pathways, which facilitate the reaction of LC3-I with the membrane lipid phosphatidylethanolamine, resulting in the formation of LC3-II on phagophore membranes [34]. Given that LC3-II formation is a marker protein for mitophagy and macroautophagy, the LC3-II is a useful tool for estimating cellular autophagic flux. We treated GFP-PRKN HEK293 cells with the top strains from the PRKN recruitment screen and tested whether LC3-II (normalized to TUBA) was potentiated in response to treatment with probiotics and CCCP. Pre-treatment with the probiotic candidates did not induce change in LC3-II level with or without CCCP (Fig. S1F,G). Paradoxically, probiotic treatment seemed to counteract the effect of chloroquine, which blocks the binding of autophagosomes to lysosomes and thus inhibits autophagy (Fig. S1F,G). These results suggest that it may be more suitable to study probiotic-mediated lysosomal degradation in an animal model rather than cellular, as the nutritional content of probiotics resulting from prolonged co-cultures may interfere with autophagy in a cell-based assay.

We have now demonstrated that the top probiotic candidates have mitophagy-promoting effects in cellular assays. However, it remains unclear whether the candidate strains will have the same effect *under* physiological conditions. We thus sought to test our top candidates in *Drosophila* PD models [35]. Of the top probiotic candidates, we tested CNCM-I-1079 and R1058. We forwent further testing on R0026 and the IBacilluS+ blend, as *Enterococcal* species,

such as *E. faecium* and *E. faecalis*, express a microbial L-dopa decarboxylase that metabolizes L-dopa into dopamine, making them an unfavorable treatment option for PD patients who are being treated with L-dopa [36,37]. We utilized a *Drosophila* model of chemically-induced oxidative stress and mitochondrial dysfunction using paraquat, a neurotoxin that causes a concentration-dependent increase in mitochondrial superoxide generation and consequentially results in compromised motor function, organismal survival, and dopamine levels in the brain [38,39]. We assessed whether mitophagy-promoting probiotics could be used to suppress these phenotypes, which are akin to those in *Drosophila* with Pink1 or park genetic mutations [14,15,40].

We used a mitochondrial quality control (mitoQC) *Drosophila* model that can be used to measure and quantify damaged mitochondria that are labeled for lysosomal degradation. To achieve this, these flies express a mitoQC transgene that fuses the transmembrane segment of the mitochondrial protein OMP25 with mCherry and GFP. This gene is selectively expressed in dopaminergic neurons using a *Drosophila* TH (tyrosine hydroxylase) *Pale* GAL4 driver, via the UAS-GAL4 system [41]. Mitochondria that have not been delivered to lysosomes appear yellow, while mitochondria that are localized within lysosomes appear red due to the pH-mediated quenching of GFP fluorescence and the stability of mCherry in acidic environments [42]. Mitolysosomal content was determined using a mitoQC analysis algorithm [43] and the percentage of cell area with a red-only signal was quantified. Optimal dosage levels of CNCM-I-1079 and R1058 were obtained from dose response curves that were generated from flies fed a range of probiotic concentrations in addition to paraquat and had their climbing ability tested (Fig. S2A,B). In flies that were fed either CNCM-I-1079 alone or CNCM-I-1079 and paraquat, there was a significant elevation in red-only regions in TH neurons compared to flies fed either paraquat alone or a water vehicle in their food (Figure 3A, E, F). Similarly, flies that were fed R1058 and paraquat showed an elevation of red-only regions in TH neurons when compared to flies fed paraquat alone or a water vehicle (Figure 3A, G, H). These results were not replicated in flies that were fed the negative control strain R0440 either alone or with paraquat, indicating that elevated mitolysosomal content was specific to CNCM-I-1079 and R1058 (Figure 3A). To demonstrate that this is a PRKN-dependent phenomenon, TH-GAL4> mitoQC flies were crossed with UAS-*park* RNAi flies to generate a park knockdown fly line. When these flies

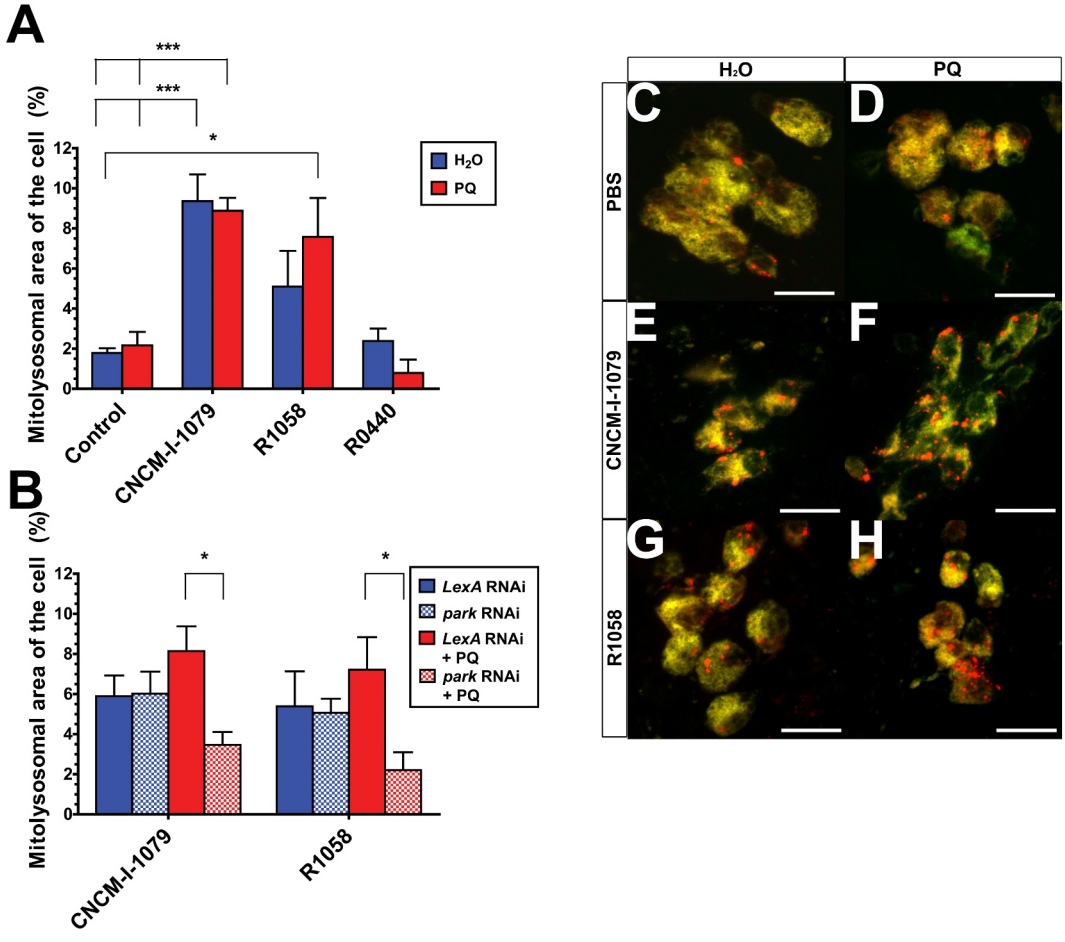

Figure 3. CNCM-I-1079 and R1058 enhanced lysosomal degradation of mitochondria in fly brain through a park-dependent mechanism. (A), percent mitolysosomal area of cells from flies stably expressing a mitochondrially-localized GFP/RFP reporter and (B) flies co-expressing the GFP/RFP reporter and either *LexA* RNAi or *park* RNAi. Flies were fed food containing a water vehicle (C), 2.5 mM paraquat (D), 3.0×10^9 CFU/mL CNCM-I-1079, 1.0×10^{10} CFU/mL R1058, or 1.0×10^{10} CFU/mL R0440 in the absence (E and G) or presence (F and H) of paraquat for 7 days and brains were then dissected, fixed, and imaged. Data are mean ± SEM (n = 4 for all groups). Asterisks represent data sets that are significantly different from baseline (* represents $p < 0.05$ and *** represents $p < 0.0001$). Scale bars: 10 μm.

were fed CNCM-I-1079 or R1058 in addition to paraquat, the probiotic-mediated elevation in mitolysosomal content in TH neurons was significantly attenuated when compared to a lexA RNAi control group (Figure 3B), indicating that the probiotic-mediated elevation in mitolysosomes during paraquat-induced mitochondrial stress is likely a PRKN-mediated phenomenon.

To test the effect of probiotics on survival, seven-day-old wild type Canton-S flies were fed a diet of fly food mixed with paraquat and either CNCM-I-1079 or R1058. Flies that were fed CNCM-I-1079 or R1058 in addition to paraquat demonstrated an improvement in longevity when compared to flies fed paraquat alone (Figure 4A, C) and feeding flies CNCM-I-1079 significantly extended the lifespan of flies when compared to flies fed a water vehicle alone (Figure 4A). To test whether probiotics also modulate motor function, seven-day-old wild type Canton-S flies were fed fly food containing probiotics and either paraquat or a water vehicle for 48 h before being tested for their climbing ability. Climbing ability was assessed by gently tapping vertical plastic vials that contained 20 flies and determining how quickly flies could climb 12.5 cm. Flies that were fed CNCM-I-1079 and paraquat, as well as flies that were fed R1058 and paraquat, both showed marked improvement in their climbing ability when compared to flies that were fed paraquat alone (Figure 4B, D). To test whether these positive effects of CNCM-I-1079 and R1058 on longevity and climbing ability are specific to those strains, we repeated longevity and climbing assays on flies fed food containing R0440, a strain that does not induce PRKN-mediated mitophagy. Flies that were fed R0440 and paraquat did not exhibit a rescue phenotype in either longevity or climbing assays compared to flies that were fed paraquat alone (Figure 4E, F). To verify that the probiotic-mediated improvement of motor function by CNCM-I-1079 and R1058 was due to neuronal mitophagy, we repeated climbing assays in flies that had park expression knocked down under the control of the brain driver *elav* using the UAS-GAL4 system. To reduce variability in climbing ability between fly lines with different genetic profiles, climbing ability was normalized to water-fed controls within each RNAi group. We found that when compared to *elav*>mCherry RNAi flies that were fed CNCM-I-1079 with paraquat, *elav*>*park* RNAi flies that were fed CNCM-I-1079 with paraquat climbed less effectively (Figure 4G), while no differences were observed in R1058 flies. While R1058 treatment was not affected by *elav*-driven *park* knockdown here, we observed reduced mitolysosome area with *TH*-driven park RNAi in flies fed paraquat and R1058 (Figure 3B), suggesting that park RNAi is less strongly expressed using the neuronal driver *elav*. Overall, these results suggest that CNCM-I-1079 likely alleviates motor dysfunction in flies through a park-mediated mechanism.

To further support the notion that probiotics impact mitochondrial health, we utilized a secondary *Drosophila* model of mitochondrial dysfunction that possesses mitochondria with both wild type and mutated mitochondrial DNA (mtDNA), a phenomenon known as heteroplasmy. Specifically, these flies possess a temperature-sensitive threonine-to-isoleucine substitution of cytochrome c oxidase subunit I (*mt:CoI*^{T300I}) that causes compromised mitochondrial electron transport, depolarized mitochondrial membrane potential, and impaired calcium uptake, which ultimately leads to neurodegeneration, impaired motor function, and reduced lifespan [44]. While homoplasmic *mt:CoI*^{T300I} flies containing 100% mutant mtDNA fail to eclose at 29°C and can only live up to 5 days when shifted to 29°C following eclosion [44] heteroplasmic flies containing ~90% mutant mtDNA exhibit a reduced but still observable impairment to motor function and longevity at 29°C [29]. Elevated heteroplasmic mtDNA variation is a hallmark characteristic of postmortem PD tissue [45] and dysfunctional autophagy in flies is correlated with an accumulation of mtDNA mutations and locomotor defects [46]. Therefore, potentiating mitophagy is one strategy to selectively reduce mtDNA mutation load and restore locomotory function, and heteroplasmic flies were used for this purpose. Heteroplasmic flies that were fed CNCM-I-1079, but not R1058, exhibited a marked recovery in motor function in comparison to heteroplasmic control flies that were fed fly food without probiotics. (Figure 4H), demonstrating that the protective benefits of probiotics are observed in different models of mitochondrial dysfunction and are not exclusive to chemical toxicity models. Further, these data demonstrate that CNCM-I-1079 is the top therapeutic candidate in *Drosophila* models of mitochondrial dysfunction.

Probiotics stimulate mitophagy via the release of small molecules, which includes methyl-isoquinoline-6-carboxylate (MI6C) and picolinic acid (PA)

The above results demonstrate a role for probiotics in the control of mitophagy. However, it is unclear how probiotics are initiating mitophagic pathways, be it through the release of small molecules or cell-cell contacts via surface macromolecules present on plasma membranes. To elucidate this further, overnight cultures of the top probiotic candidates were generated and separated into supernatant/cellular fractions, and the cellular fractions were killed via heat. These fractions were first tested for their ability to induce mitophagy using the GFP-PRKN cell assay: CCCP-treated cells that were incubated in media containing up to 80% supernatant from R0026, CNCM-I-1079, R1058, and the IBacilluS+ blend resulted in a dose-dependent significant increase in mitochondrial PRKN recruitment, while supernatant fractions from R0179 did not (Figure 5A). These results were not observed in cells that were incubated in media containing 80% supernatant and treated with a DMSO vehicle, indicating that supernatant fractions do not induce mitophagy in the absence of CCCP. Cell media that contained more than 80% supernatant resulted in a loss of HEK293 cell adherence and these data were therefore not quantified. Dead cell fractions did not significantly change CCCP-mediated PRKN recruitment for any of the strains tested, with the exception of the IBacilluS+ blend which caused a significant increase in PRKN recruitment at an MOI of 100:1, but not 50:1 or 10:1. Dead cells from the components of the IBacilluS+ blend (R0179 or R0026) alone did not induce PRKN recruitment at any MOI (Figure 5B), suggesting that either expression of cell surface macromolecules of these strains may be affected by mutualistic interactions, or mitophagy-inducing metabolites that are

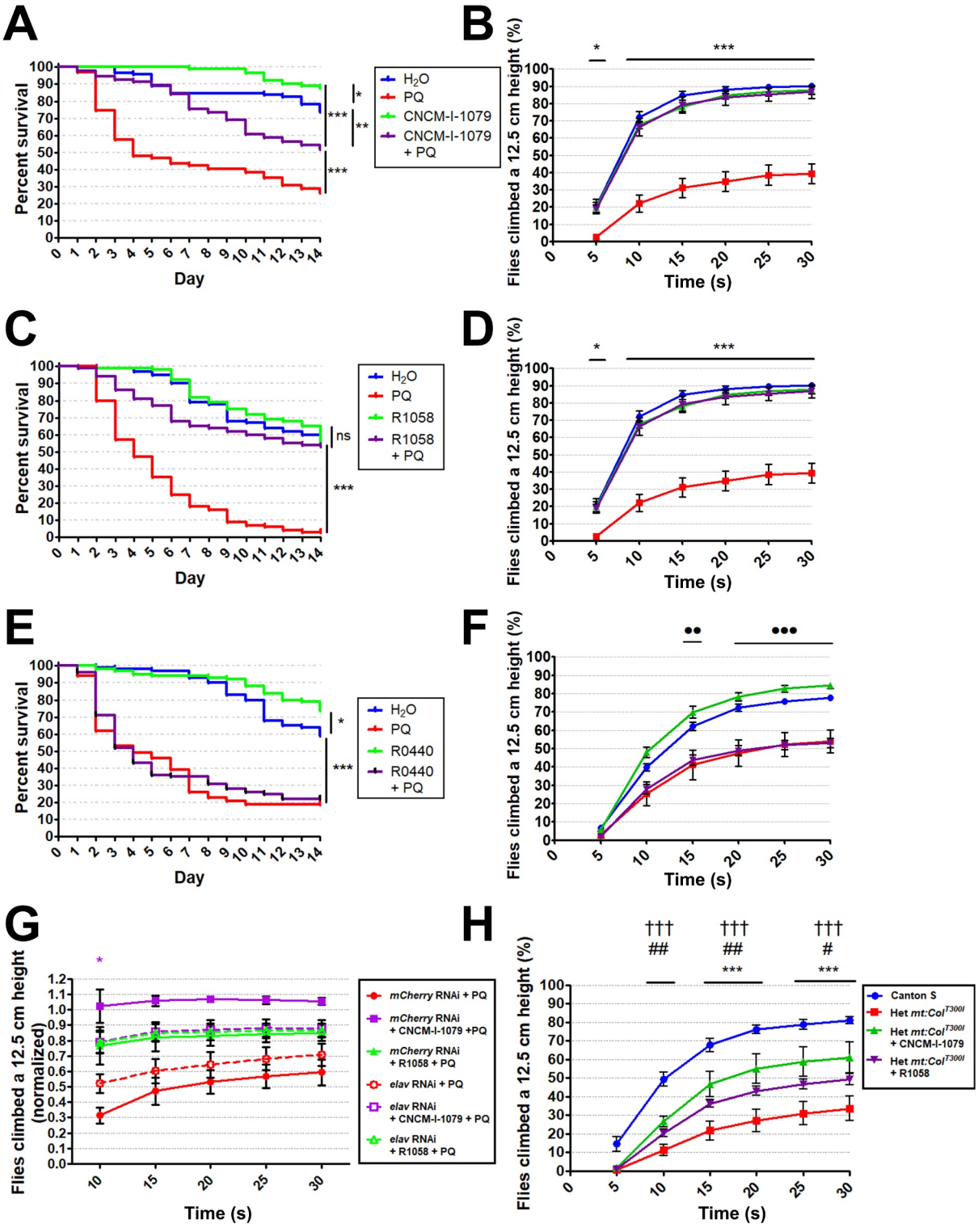

Figure 4. Survival and climbing defects as a result of paraquat-mediated mitochondrial dysfunction are improved by CNCM-I-1079 and R1058. Canton (S) flies were fed food that was supplemented with either a water vehicle, paraquat (2.5 Mm5E), probiotics alone, or probiotics and paraquat (2.5 mM). Flies were given treated food on day 0 for survival assays and for 48 h prior to climbing experiments. Survival and climbing assays were conducted for CNCM-I-1079 (A and B) at 3.0×10^9 CFU/mL) R1058 (C and D) at 1.0×10^{10} CFU/mL), and R0440 (E and F) 1.0×10^{10} CFU/mL). (G), *elav>park* RNAi and *elav>mCherry* RNAi flies were fed combinations of a water vehicle, paraquat, or probiotics CNCM-I-1079 or R1058 with PQ. **H**, heteroplasmic flies that were fed control fly food or fly food containing CNCM-I-1079 or R1058 for 6 days before climbing. All data are represented as the mean ± S.E.M. (n = 100 for survival groups and n = 5 for all climbing groups). For Canton-S/RNAi climbing assays, an asterisk (*) indicates a statistically significant difference between the paraquat and probiotic-fed group and the paired paraquat group and a circle (●) indicates a significant difference between water control and the paraquat/probiotic-fed groups. For heteroplasmic climbing assays, a cross (†) represents a significant difference between Canton-S flies and heteroplasmic flies, a number sign (#) indicates a significant difference between Canton-S flies and heteroplasmic flies fed CNCM-I-1079, and an asterisk (*) represents a significant difference between control heteroplasmic flies and heteroplasmic flies fed CNCM-I-1079 (where one symbol represents $p < 0.05$, two represents $p < 0.01$, and three represents $p < 0.0001$).

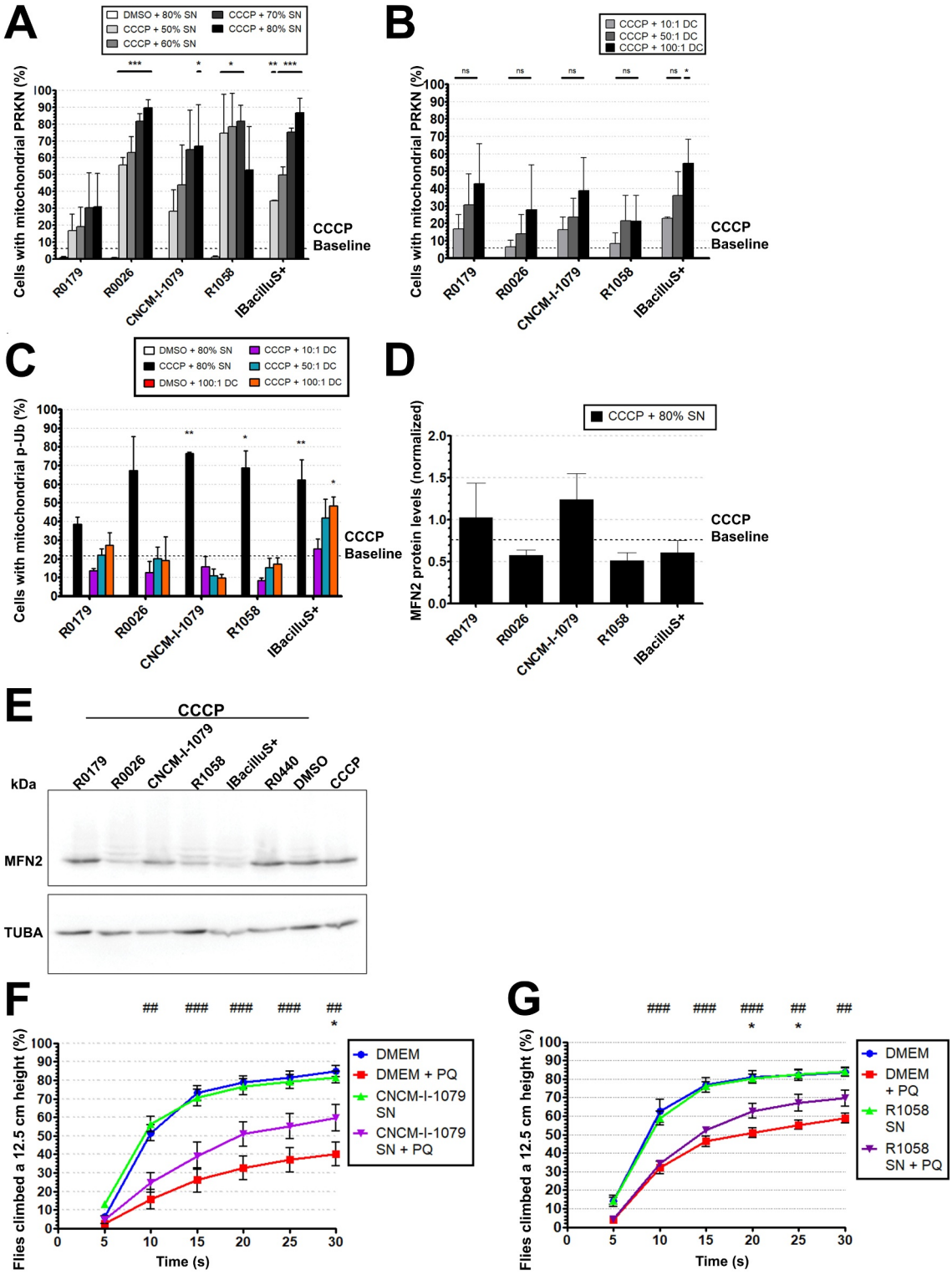

Figure 5. Supernatant fractions from candidate strains regulate the mitophagic response. Mitochondrial PRKN recruitment in CCCP-treated HEK293 cells (6.0 μM, 2 h) in response to preincubation with probiotic supernatant fractions (**A**, 50–80% of cell media) and dead cells (**B**, MOIs of 100:1, 50:1, and 10:1). The dotted line represents baseline PRKN recruitment following CCCP stress in the absence of any additional treatments. p-Ub expression (C) and MFN2 degradation (D) was also measured in CCCP-treated HEK293 cells (6.5 μM, 2 h and 1.5 h, respectively) that were pre-incubated with 80% supernatant fractions or dead cells. Sample western blot for cells exposed to probiotic supernatant fraction and CCCP is shown (E). Climbing assays were conducted in flies that were fed food that was mixed with 50% supernatant samples in the absence of live cultures for CNCM-I-1079 (F), and R1058 (G). All data are represented as the mean ± S.E.M. (n = 3 for all cell-based groups in **A-D**, n = 5 for all climbing experimental groups in **F-G**). An asterisk indicates a statistically significant increase from baseline in the absence of probiotic pre-incubation and, for climbing assays, a number sign indicates a statistically significant difference between the paraquat and probiotic-fed group and the paired water control group (where one symbol represents $p < 0.05$, two symbols represent $p < 0.01$, and three symbols represent $p < 0.0001$).

released by R0179 and R0026 blends cannot be effectively removed from dead cell fractions.

To further investigate probiotic fractions, we tested whether supernatant or dead cell fractions promoted mitochondrial phospho-ubiquitination and MFN2 degradation. Similar to the PRKN recruitment screen, supernatant samples significantly elevated p-UB expression in CCCP-treated cells that were pre-incubated with CNCM-I-1079, R1058, and the IBacilluS+ blend but not R0179 and R0026 (Figure 5C). Dead cell treatment was only effective for the IBacilluS+ blend at an MOI of 100:1 but not 50:1 or 10:1. However, supernatant samples did not significantly promote MFN2 degradation for any of the strains, suggesting that the supernatant fraction's efficacy of inducing mitophagy is less than that of live cultures (Figure 5D,E).

To determine whether supernatant solution exposure is sufficient to promote protection from chemically-induced mitochondrial dysfunction, we exposed Canton-S flies to food that contained 50% supernatant samples from CNCM-I-1079 or R1058, which was the maximum supernatant volume that could be added to fly food without liquifying it. Flies were given supernatant-treated or DMEM vehicle-treated food with either paraquat or a water vehicle and their climbing ability was assessed. Flies that were exposed to paraquat and supernatant samples from either CNCM-I-1079 or R1058 showed a marked improvement in their motor ability compared to flies that were fed paraquat alone, which indicates that the presence of live probiotic cells is not required for their protective effects to occur in *Drosophila* (Figure 5F-G). From these data, we conclude that the active mitophagy-inducing moiety of probiotic cultures is at least one molecule that is produced under laboratory conditions, is not a membrane-associated or intracellular component, and is released into the extracellular media.

We next sought to identify the molecules that are released from probiotics and whether they promote mitophagy under conditions of mitochondrial stress. High performance liquid chromatography was performed on supernatant samples from both CNCM-I-1079 and R1058 and the resulting chromatograms were analyzed. Both samples yielded similar elution patterns (Fig. S3A,B) and from these we were able to collect 7 fractions from CNCM-I-1079 samples and 6 fractions from R1058 samples. These fractions were tested for activity using the GFP-PRKN assay. 6 of the 7 fractions from CNCM-I-1079 and fractions 2, 3, 4, and 5 from R1058 significantly increased mitochondrial PRKN recruitment in CCCP-treated cells, while fraction 1 from both strains resulted in quenching of the GFP-PRKN signal (Fig. S3D,E). Each of these fractions was analyzed via ultraperformance liquid chromatography-tandem mass spectrometry to elucidate the molecular identity of each fraction. We were able to identify 3 molecules from these samples: fraction 1 from both strains contained melanoxadin (Fig. S4), fraction 2 from both strains contained PA (Fig. S5A,B), and fraction 5 from both strains contained MI6C (Fig. S6A,B). The remaining fractions contained multiple molecules and their individual identities could therefore not be identified. Given that melanoxadin is incompatible with our GFP-based mitophagy assays due to its evident GFP-quenching characteristics, we sought to identify whether PA or MI6C are involved in mitophagy induction.

To verify whether PA and/or MI6C are involved in potentiating mitophagy, we tested the capacity of each chemical to enhance mitophagy using the previously described cell assays. MI6C potentiated mitochondrial PRKN recruitment in CCCP-treated cells with an EC_{50} of 79.97 μM (Figure 6A), whereas PA potentiated PRKN recruitment at higher dosages with an EC_{50} at 3.894 mM (Figure 6B). MI6C significantly increased Ser65-pUb levels in GFP- PRKN HEK293 cells at 1 mM and 500 μM, while PA had no effect on p-Ub levels at either 1 mM or 5 mM (Figure 6C). However, both MI6C (1 mM) and PA (5 mM) significantly reduced MFN2 levels following CCCP stress when compared to cells treated with CCCP alone (Figure 6D), while neither molecule induced a significant reduction of MFN2 levels or led to severe mitochondrial fragmentation without CCCP-induced mitochondrial stress (Figure 6D, Fig. S5C-D, Fig. S6 C-D). MI6C significantly increased LC3-II:LC3-I ratios in cells treated with DMSO but not CCCP and PA had no effect (Fig. S1H, G), suggesting that MI6C is involved in upregulating early- and late-stage mitophagy. Isoquinoline derivatives have been implicated to inhibit complex I of the electron transport system due to their structural similarity to 1-methyl-4-phenyl-1,2,3,6-tetrahydropyridine (MPTP) and may thus be endogenous neurotoxins that could promote neurodegeneration and PD onset [47]. Given that complex I inhibition may lead to mitochondrial membrane potential destabilization and mitochondrial damage, we sought to test the potential of MI6C as a modulator of mitochondrial membrane potential and to verify whether this is a causative factor for mitophagy induction in the absence of CCCP. HEK293T cells were incubated with MI6C or a DMSO vehicle for 24 h to assess whether prolonged exposure to MI6C depolarized mitochondrial membrane potential and this was assessed using the mitochondrial membrane potential-sensitive dye JC-1 via flow cytometry. JC-1 is a lipophilic, cationic dye that naturally exhibits green fluorescence. In healthy, negatively charged mitochondria, JC-1 accumulates, and forms reversible complexes called J aggregates that fluoresce in the red spectrum while, conversely, J aggregates do not form in mitochondria that are damaged/depolarized and therefore JC-1 retains its original green fluorescence under these conditions. Therefore, the ratio of red:green fluorescence can be utilized to assay the status of mitochondrial membrane potential [48]. Cells that were treated with CCCP exhibited a lowered red:green fluorescence ratio than cells treated with a DMSO vehicle, and the red:green fluorescence ratio from cells treated with MI6C was significantly higher than that in cells treated with CCCP (Figure 6E). These data suggest that MI6C does not potentiate mitophagy by mitochondrial depolarization.

To assess whether there are protective effects of MI6C and PA in flies, we first performed a dose response climbing experiment to test each metabolites efficacy in offsetting paraquat-mediated motor dysfunction. Concentrations ranging from 10 μM–1 mM were tested for MI6C, while 500 μM–10 mM were tested for PA (Fig. S2C,D). Flies that were fed 100 μM MI6C showed a significant improvement in climbing ability (Figure 6F), while flies that were fed PA did not show

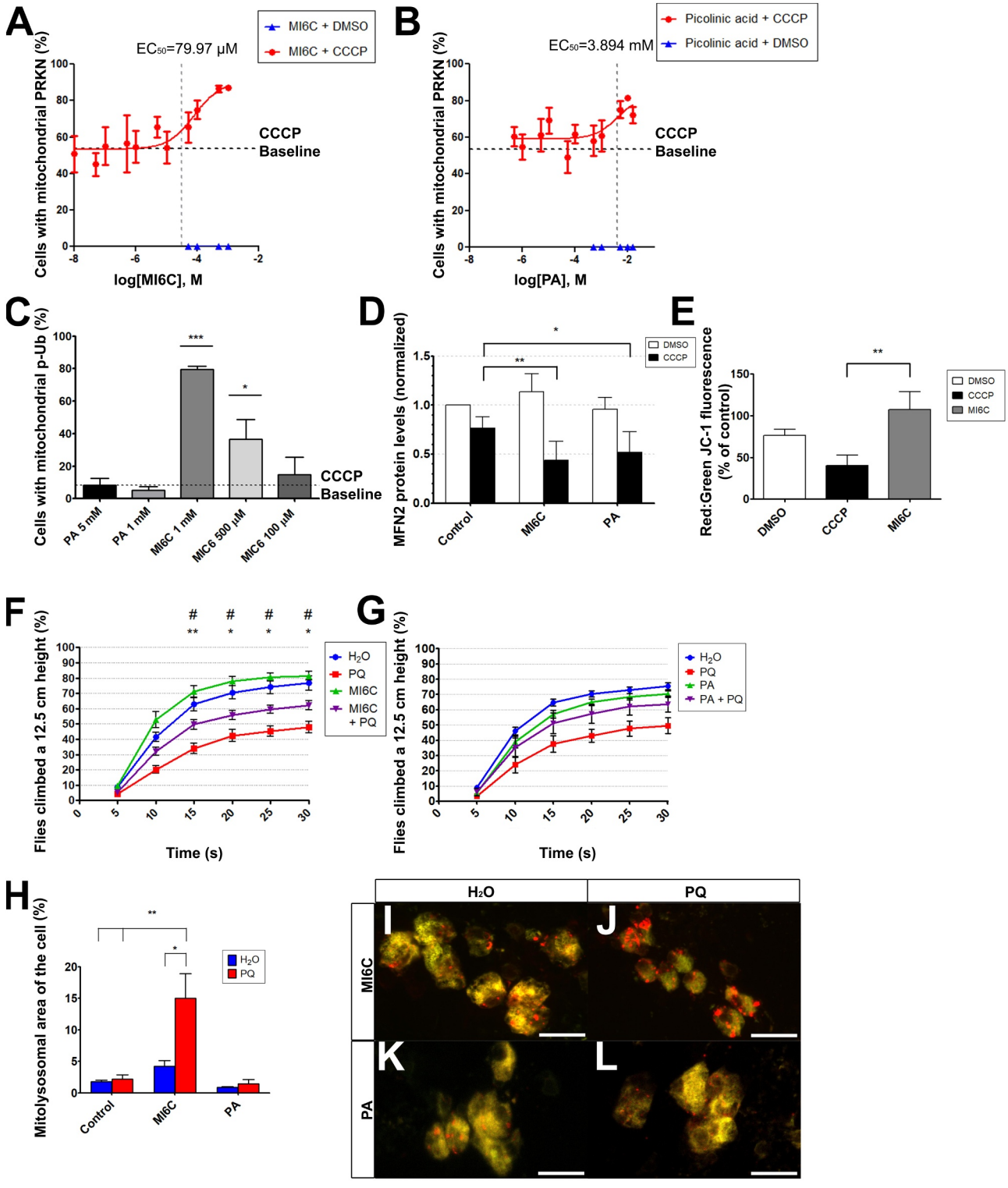

Figure 6. Methyl-isoquinoline-6-carboxylate (MI6C), but not picolinic acid (PA), promoted mitophagy induction. PRKN recruitment dose-response curves with EC_{50} values for (A) MI6C and (B) PA, (C) Ser65-pUb assays, and (D) MFN2 assays were conducted in GFP-PRKN HEK293 cells after being treated with MI6C or PA following by CCCP. MFN2 data are expressed as the ratio of MFN2:TUBA band density, divided by the MFN2:TUBA ratio band density obtained from cells exposed to DMSO only. (E), JC-1 fluorescence ratios of red:green fluorescence, normalized to fluorescence ratios from cells that were only treated with JC-1. Climbing assays were conducted in flies fed MI6C (F) or (G) PA with or without PQ for 48 h prior to experimentation. (H) lysosomal degradation of mitochondria in the brain of flies stably expressing a mitochondrially-localized GFP/RFP reporter that were fed MI6C (I and J) or PA (K and L) in the absence or presence of PQ, respectively. All data are mean ± SEM (n = 3 for PRKN recruitment and p-Ub assays, n = 6 for MFN2 assays, n = 4 for JC-1 assays, n = 5 for climbing assays, n = 4 for mitoQC experiments. Asterisks represent data sets that are significantly different from baseline (* represents $p < 0.05$, ** represents $p < 0.01$, and *** represents $p < 0.001$). Scale bars: 10 µm.

any apparent improvement to motor function at any concentration that was tested and no observed significant differences at the highest concentration (Figure 6G). To test whether these molecules regulate mitophagy in dopaminergic neurons, we fed each molecule to flies expressing the mitoQC transgene that was under the control of a TH driver. Flies that were fed MI6C and paraquat showed a 7-fold increase in areas corresponding to mitochondrial degradation via lysosomes, compared to flies fed paraquat alone (Figure 6H, J). Feeding flies MI6C alone did not result in an increase to mitolysosomal area, indicating that MI6C alone does not induce mitophagy (Figure 6H, I). Taken together, these results indicate that MI6C is a small molecule that probiotics release that can influence mitochondrial autophagy and turnover.

Discussion

In this study we have identified probiotics that can stimulate PRKN-dependent mitophagy and, of those tested, *Saccharomyces boulardii* (CNCM-I-1079) and *Lactococcus lactis* (R1058) were most effective. *S. boulardii* and *L. lactis* both promoted mitophagy across all assays utilized in this study, which include mitochondrial PRKN recruitment, phospho-ubiquitination, and MFN2 degradation in GFP- PRKN HEK293 cells, and promoted lysosomal degradation, improved motor function, and increased lifespan in flies. However, *L. lactis* failed to improve the motor phenotype of heteroplasmic flies, which leaves *S. boulardii* as the top mitophagy-promoting candidate in this study. This is the first study which demonstrates that *S. boulardii* and *L. lactis* positively promote mitophagy in any biological model. *Lactobacillus rhamnosus* GR-1 has been implicated in promoting PINK1- and PRKN-mediated mitophagy [49], however we did not observe elevated mitochondrial PRKN recruitment induced by any strains of *L. rhamnosus* that were tested here.

We utilized GFP-PRKN HEK293 cells as the primary *in vitro* model for our study. While overexpression of PRKN can potentially distort the relative level of endogenous PINK1-PRKN-dependent mitophagy, specifically in cases where there is a mitophagy deficiency caused by a loss of PINK1 [50,51], the purpose of this study was to investigate whether probiotics can modulate PRKN activity in CCCP-treated cells beyond an experimental control baseline. We have demonstrated a clear connection between probiotics and PINK1-PRKN-dependent mitophagy, as evidenced by elevated mitochondrial PRKN recruitment in the presence of probiotics and CCCP, and an absence of recruitment in co-cultures not exposed to CCCP. However, these effects may be less dramatic under physiological conditions, where PRKN expression is expected to be much lower.

We sought to determine the molecular identity of mitophagy-inducing components in *S. boulardii* and *L. lactis* cultures to further elucidate their mechanism of action. We have identified 3 molecules in this study that exist in cultures of both strains under laboratory conditions: melanoxadin, PA, and MI6C. While we were unable to study the effects of melanoxadin on mitophagy due to the GFP-quenching nature of melanoxadin-containing fractions, its function is implicated in dopamine biosynthesis. Melanoxadin inhibits melanin biosynthesis in larval silkworm hemolymph [52] and it bears a structural similarity to melanoxazal, an inhibitor of tyrosinase [53]. Tyrosinase catalyzes the conversion of L-tyrosine to L-DOPA and contributes to the formation of neuromelanin in dopaminergic neurons of the substantia nigra [54]. While neuromelanin is thought to protect neurons from redox-active metals and toxins, it cannot be degraded intracellularly and thus accumulates over a lifetime. Tyrosinase overexpression and neuromelanin accumulation in rat substantia nigra is associated with an age-dependent PD phenotype, which includes hypokinesia, Lewy body formation, and neurodegeneration [55]. It may therefore be possible that probiotic-mediated melanoxadin production could lead to lower levels of neuromelanin production and mitigation of progressive neurodegeneration. The second released molecule in our study, picolinic acid, is a pyridine monocarboxylic acid that is a product of tryptophan metabolism through the kynurenine pathway, a pathway that generates nicotinamide adenine dinucleotide (NAD). Prolonged picolinic acid exposure leads to generation of elongated, electron-dense mitochondria, which was suggested to occur as a result of bivalent iron chelation and disruption of mitochondrial iron metabolism [56]. Given that high concentrations of picolinic acid chelate iron [56] and iron deficiency triggers mitophagy [57], it is possible that the high concentrations of picolinic acid (1–5 mM) that were effective at inducing mitophagy in this study did so by disrupting mitochondrial iron metabolism.

The most potent molecule of this study that potentiated mitophagy is MI6C, which potentiated PRKN recruitment, mitochondrial phospho-ubiquitination, and MFN2 degradation in CCCP-treated cells and promoted mitolysosomal degradation and improved locomotory ability in paraquat-treated flies. No previous study has demonstrated the existence of MI6C in metabolomic data from the GI tract. However, isoquinoline derivatives were shown to exist in a variety of biological sources including dairy products [58]. The amino acid tyrosine, commonly found in the GI tract, is a precursor for isoquinoline biosynthesis. One of the first enzymes involved in the biosynthesis pathway is tyrosine decarboxylase [59]. Bacteria from the genus *Lactococcus*, including species of *L.lactis*, were shown to be able to produce tyrosine decarboxylase [60], suggesting a possibility for *L. lactis* R1058 to biosynthesize isoquinoline derivatives through the tyrosine pathway. It is also worth noting that MI6C is listed as irritant to skin, eyes, and respiratory tract (ECHA), suggesting that further investigation is needed to identify the therapeutic concentration for MI6C or to explore the potential for MI6C to be used as a starting scaffold for synthesizing of other isoquinoline derivatives that are more suitable therapeutics [61]. Isoquinoline derivatives have been found to reduce mitochondrial respiration by inhibiting complex I activity, an effect that was compared to the neurodegenerative effects of MPTP [47]. Sustained inhibition of complex I with rotenone resulted in mitochondrial hyperpolarization [62], however we saw that mitochondrial membrane potential was maintained in the presence of MI6C suggesting that it does not effectively hyperpolarize membrane potential via complex I inhibition in intact HEK293 cell mitochondria.

However, inhibition of complex I has been shown to induce autophagosome formation and mitophagy [63], which is consistent with the slightly elevated LC3-II level that we observed following MI6C exposure to cells. It remains unclear however whether probiotics release MI6C at concentrations high enough to compromise complex I activity under physiological conditions. At lower concentrations, moderate inhibition of complex I may offer protection to cells through the concept of mitohormesis, whereby a mild sub-lethal mitochondrial stress activates cytoprotective pathways that protect against larger, subsequent stresses [64]. Pharmacological inhibition of complex I at 0.1% of its LD_{50} led to prolonged longevity in killifish [65], as did genetic knockdown of complex I in *Drosophila* [66]. While complex I deficiency in substantia nigra is a central component to PD, neuronal complex I loss is not correlated with mtDNA damage and is inversely correlated with alpha-synuclein aggregation [67]. These results suggest a potential biphasic response with complex I inhibition, which may apply to the mode of action of MI6C in this study. Given that we did not see PRKN recruitment in cells that were incubated with MI6C in the absence of CCCP, it suggests that MI6C may regulate mitophagy at multiple stages beyond complex I, as MI6C is shown to induce mild mitochondrial fission (Fig. S6C), which can potentially lead to induction of mitophagy [68,69]However, further studies are needed to identify the mechanism of how MI6C is involved in the regulation of mitochondrial fission/fusion. One additional route of mitophagy regulation could be via inhibition of the Rho/ROCK pathway, as the isoquinoline derivative berberine inhibits the Rho/ROCK pathway in rats [70] and ROCK inhibitors potentiate PRKN-mediated mitophagy in CCCP-treated cells [29]. LC-MS of homogenates taken from whole *Drosophila* fed with probiotic supplemented food did not reveal peaks identical to the peaks detected in the MI6C standard (data not shown). This suggests that under physiological conditions, administration of probiotic-supplemented food did not lead to the production of MI6C in flies at a detectable concentration. It is worth noting that in addition to the molecules that we identified, there are likely numerous molecular species converging on mitochondrial and mitophagy pathways. One example is the short-chain fatty acid butyrate, which is elevated in the stool samples of patients fed *S. boulardii* [71]. Butyrate enhances PRKN recruitment to mitochondrial fractions and leads to a reduction in mitochondrial mass in hamster ovary cells [72], and also upregulates expression of genes associated with mitochondrial fission and mitophagy, which includes DRP1, PINK1, LC3, and PTEN [73].

The beneficial effects of *S. boulardii* go beyond the current study: it has been demonstrated to alleviate diarrhea in tube-fed patients [74] and treat symptoms of ulcerative colitis and inflammatory bowel disease in rodents [75,76]. Its mechanism of action is multifold: it supports the growth of beneficial intestinal bacteria by providing substrates for fermentation via its cell wall [71,77], reduces inflammation by attenuating the release of pro-inflammatory cytokines [76], and limiting the migratory behavior of T-cells [75] while also releasing enzymes involved in nutrient digestion that service the host [78]. *L. lactis* has also been implicated in relieving inflammatory disease: the *L. lactis* strain NCDO 2118 reduces inflammatory cytokine production in intestinal cells [79]. More importantly to this study, *L. lactis subsp. lactis* upregulates AMPK signaling [80], which enhances mitochondrial fission by phosphorylating mitochondrial fission factor and promotes mitophagy independently of PINK1 and PRKN [81]. Given that probiotics have can possess anti-inflammatory properties in addition to the mitophagy-promoting properties observed in this study, they may be a prophylactic solution for early-stage PD patients who are experiencing intestinal distress. Future studies should investigate whether the mitophagy-modulating effects of *S. boulardii* and *L. lactis* are preserved in mammalian models.

Materials and methods

Cell lines/cell culture

HEK293 cells that stably expressed GFP-PRKN were used in this study and their development has been described [29]. HEK293 cells were cultured in Dulbecco's modified Eagle's Medium (DMEM; Corning, 10–017-CV) that was supplemented with 10% fetal bovine serum (Thermo Fisher Scientific/Gibco,12,483–020) at 37°C in humidified air that contained 5% CO_2.

Probiotic preparation

The 49 probiotic microbes or combinations of microbes that were tested were obtained from Lallemand Health Solutions (Table S1) as lyophilized powders with a predetermined concentration (colony-forming units [CFU]/g). Probiotic powders were resuspended in PBS to a concentration of 9.4×10^7 CFU/mL, where the probiotic specific PBS was composed of 0.1% peptone (BioShop Canada Inc., PEP403.1), 0.121% dipotassium hydrogen phosphate (ACP Chemicals INC., P-4545), and 0.034% potassium dihydrogen phosphate (BioShop Canada Inc., PPM302.1), pH 7.4. Probiotic suspensions were placed on a shaker for 15 min at room temperature (≈22°C) before being used for experimentation. Each of the 49 probiotic samples were assigned a number prior to the screen and were identified only by that number during the screen to reduce experimenter bias (Table S1).

Supernatant and dead cell preparation

Lyophilized probiotic powders were resuspended in DMEM to a final concentration of 1.9×10^8 CFU/mL and were left to grow on a shaker for 24 h at 37°C and 220 rpm. The resultant cultures were centrifuged at 18,928 x g for 10 min and the supernatant was transferred to a clean tube, where its pH was adjusted to 7.0 with acetic acid (Caledon Laboratory Chemicals, 1000-1-29). Final supernatant solutions were filtered through a 0.22 µm syringe filter (Pall Corporation, 4612) and were then swabbed on LB agar plates (20 g/L agar [Bioshop Canada Inc., AGR003.1], 10 g/L NaCl [BioShop Canada Inc., SOD002.205], 10 g/L tryptone [BioShop Canada Inc., TRP402.5], 5 g/L, yeast extract [BioShop

Canada Inc., TEX401.500]) and incubated at 37°C for 48 h to verify an absence of growth. The pellet from centrifuged overnight cultures was washed three times in probiotic specific 1x PBS and was autoclaved for 15 min at 121°C to produce a dead cell solution. Dead cells were swabbed onto a LB agar plate and incubated at 37°C for 48 h to verify an absence of growth. All steps were done adjacent to an open flame to minimize contamination.

GFP-PRKN HEK293 probiotic screening

Glass-bottom 96-well plates (Eppendorf, 0030741030) were coated with 0.1 mg/μL poly-D-lysine (Sigma-Aldrich, P0899) for 30 min, washed with ddH_2O, and dried for at least 2 h in a biosafety cabinet. GFP-PRKN HEK293 cells (10,000) were seeded in each well and were given 24 h to adhere to the plate before being exposed to probiotic cultures.

GFP-PRKN HEK293 cells were either treated with a 1x PBS vehicle or were co-cultured with probiotic cells for 3 h at 37°C and 5% CO_2 using three MOIs: 100:1, 50:1, and 10:1. Media was then aspirated and replaced with either media containing 6.0 μM CCCP (Sigma-Aldrich, C2759) or a DMSO (Sigma-Aldrich, 472,301) vehicle for 2 h, after which cells were fixed in 4% PFA (Thermo Fisher Scientific, J19943-K2) for 20 min, incubated in 1 μg/mL DAPI (Roche Diagnosrics GmbH, 10,236,276,001) for 10 min, and washed in 1x PBS (1.86 mM NaH_2PO_4, 8.41 mM Na_2HPO_4, 175 mM NaCl, pH = 7.4). Plates were stored at 4°C until imaging was conducted.

Cells were imaged using a 20x dry immersion objective on a Leica SP8 confocal microscope in stacks composed of 5–6 1.5 μm slices at a resolution of 2048 × 2048 pixels and maximum projections of these stacks were compiled to produce images for analysis. Images were assigned non-descript numbers and were analyzed using Cell Profiler and Cell Profiler Analyst by a blinded individual to eliminate examiner bias. Probiotics that induced the highest level of PRKN recruitment were considered mitophagy activators and strains that induced PRKN recruitment that was significantly different from baseline at a 100:1 MOI were chosen for further analysis.

Phospho-ubiquitin immunostaining assay

65,000 GFP-PRKN HEK293 cells were seeded on poly-D-lysine-treated coverslips in 24-well plates and were incubated for 24 h. GFP-PRKN HEK293 cells were co-cultured with probiotics for 3 h at 37°C and 5% CO_2 at MOIs of 100:1, 50:1, and 10:1, and the media was then aspirated and replaced with either media containing 6.5 μM CCCP or a DMSO vehicle for 2 h. Cells were fixed in 4% PFA for 20 min, washed in 1x TBS (50 mM Tris [BioShop Canada Inc., TRS001.5], 150 mM NaCl [BioShop Canada Inc., SOD002.205], pH 7.4) 3 times, incubated in 0.1% Triton X-100 (Sigma-Aldrich, X100) for 15 min, washed in 1x TBS 3 times, blocked with 10% goat serum (Thermo Fisher Scientific Gibco, 16,210–064) for 30 min, and were then incubated in 1° Ser65-phospho-ubiquitin antibody (1:500) at 4°C on a shaker overnight. Coverslips were washed 3 times with 1x TBS and were incubated with Alexa Fluor 568 2° antibody (1:500) in 1x TBS for 2 h at room temperature. Coverslips were washed 3 times with 1x TBS, mounted with Fluoromount G (Southern Biotech, 0100–01) containing 1 μg/mL DAPI. Images were taken using a 40x oil immersion objective (Zeiss Axio Imager Z1), camera (Hamamatsu Orca-ER, C4742-80), and Volocity software. Images were analyzed using ImageJ.

MFN2 and LC3 immunoblotting

GFP-PRKN HEK293 cells were co-cultured with probiotics in 12-well plates for 3 h at 37°C and 5% CO_2 at MOIs of 100:1, 50:1, and 10:1. For MFN2 experiments, DMEM media was then aspirated and replaced with media containing 6.5 μM CCCP or a DMSO vehicle for 90 min. For LC3 experiments, cells were exposed to either 10 μM CCCP, 10 μM CCCP and 50 μM chloroquine, for a DMSO vehicle for 4 h. Cells were washed with 1x PBS. Lysis buffer (20 mM Tris, 300 mM NaCl, 1 mM EDTA [BioShop Canada Inc., EDT001.500], 2 mM EGTA [BioShop Canada Inc., EGT101.50], 10 Mm $MgCl_2$ [BioShop Canada Inc., MAG510.500], 1% Triton X-100, 1% SDS [BioShop Canada Inc., SDS001.1],pH 7.4) was then added, and cells were scraped off the plate and incubated on ice for 30 min, and then centrifuged at 16,128 x g for 20 min at 4°C. The supernatant was moved to a new tube for protein quantification via BCA assay (Thermo Fisher Scientific, 23,227). Samples were boiled for 15 min at 95°C and were run on 8% SDS-PAGE gels (Resolving gel, 8% acrylamide [Bio-Rad Laboraties, 1,610,158], 25% 1.5 M Tris, pH 8.8, 0.1% SDS, 0.1% ammonium persulfate [Bio-Rad Laboraties, 1,610,700], 0.06% TEMED [BioShop Canada Inc., TEM001.25]; Stacking gel, 5% acrylamide, 12.6% 1 M Tris, pH 6.8, 0.1% SDS, 0.1% ammonium persulfate, 0.1% TEMED). and transferred onto PVDF membranes (Millipore Sigma, IPVH00010) at 400 mA for 90 min. Membranes were blocked in 5% skim milk (dissolved in 1XTBST; BioShop Canada Inc., SKI400.500) and 1x TBST (1x TBS and 0.1% Tween-20 [BioShop Canada Inc., TWN510.500]) for 20 min at room temperature and incubated in either 1° MFN2, 1° LC3, or 1° TUBA antibodies (1:2000) overnight. Blots were incubated in HRP 2° antibody (1:2000) for 1 h and visualization was achieved using an ECL luminescence kit (Bio-Rad, 11,705,062). Densitometry analysis was performed using ImageLab 6.1 software (Bio-Rad) and protein bands were normalized to an internal TUBA loading control. All antibodies used for western blotting were diluted in 5% skim milk.

Supernatant fractionation and LC-MSF

Supernatant fractions from *S. boulardii* (CNCM-I-1079) and *L. lactis* (R1058) overnight cultures were prepared in DMEM, centrifuged at 18,928 x g for 10 min and the aqueous fraction was collected. An equivalent volume of methanol (Fisher Chemical, A452-4) was added, and solutions were sonicated for 30 min at 35°C. Samples were dried by centrifugal evaporation (Genevac) and were resuspended to 100 mg/mL with HPLC-grade 1:1 (v:v) water:acetonitrile + 0.1% formic acid (Fisher Chemical, LS120-212). Samples were fractionated by HPLC (Alliance 2695 System, Waters)

using an XSelect C18 column (250 mm x 10 mm, 5 μm; Waters), with solvents: (A) Water + 0.1% formic acid (Thermo Fisher Scientific, 85,178), and (B) acetonitrile + 0.1% formic acid, and a 35°C column temperature. A flow rate of 0.5 or 1 mL/min was used with the following gradients: 5% B over 1 min, 5% to 95% B over 15 min, and 95% to 5% B over 4 min. Fractions were collected, dried and resuspended in 1:1 (v:v) water:acetonitrile + 0.1% formic acid for ultraperformance liquid chromatography-tandem mass spectrometry (UPLC-MS) analysis. Each fraction was analyzed on an Acquity I-Class UPLC coupled to a Waters Xevo G2-S QToF in positive ESI mode with an Acquity UPLC BEH C18 column (2.1 x 50 mm, 1.7 μM) at 40°C with a flow rate of 0.2 mL/min. The following gradient was used with solvents (A) water + 0.1% formic acid and (B) acetonitrile + 0.1% formic acid: 5% B over 1 min, 5% to 95% B over 15 min, and 95% to 5% B over 4 min. Molecules were identified with the Dictionary of Natural Products and confirmed by MSe fragmentation (Waters).

JC-1 fluorescence measurements

HEK293T cells were seeded in 12-well plates and exposed to either MI6C, or a DMSO vehicle for 24 h, where DMSO concentrations did not exceed 0.5%. CCCP treated cells were exposed to 50 μM CCCP for 5 min and all cells were then incubated with 2 μM JC-1 for 30 min. Cells were analyzed using a LSR II (BD) flow cytometer with a 488 nm argon laser and 530/30 and 576/26 nm filters. Data was processed using FACSDiva 8.0.1 software.

Chemicals

The following chemicals were used in this study: Poly-D-lysine (Sigma- Aldrich, P0899), CCCP (Sigma-Aldrich, C2759), methyl-isoquinoline-6-carboxylate (MI6C; ChemScene, CS-0021457), picolinic acid (PA; Sigma-Aldrich, P42800), paraquat (Sigma-Aldrich, 36,541), protease inhibitor cocktail (BioShop Canada Inc., PIC002), 5,5′,6,6′-tetrachloro -1,1′,3,3′-tetraethylbenzimi-dazolylcarbocyanine iodide (JC-1; Thermo Fisher Scientific, T3168), chloroquine (Tocris Bioscience, 4109).

Antibodies

The following antibodies were used in this study: rabbit anti-phospho-ubiquitin Ser65 (Sigma-Aldrich, ABS1513-I; lot: 3,587,100, 1:500), rabbit anti-MFN2/mitofusin 2 (Abcam, ab205236; lot: GR295525-7, 1:2000), rabbit anti-LC3B (Cell Signaling Technology, 2775S; lot 13, 1:2000), mouse anti-ATP5F1A/ATP5A (Abcam, ab14718; 1:500), mouse anti-TUBA/α-tubulin (Santa Cruz Biotechnology, sc-53,646; lot: G2919, 1:2000), goat anti-rabbit Alexa Fluor 568 (Life Technologies, A11011; lot: 2,017,252, 1:500), peroxidase-conjugated AffiniPure goat anti-rabbit IgG (HRP) (Jackson Immuno Research Laboratories, 111–035-045; 1:2000), peroxidase-conjugated AffiniPure goat anti-mouse IgG (HRP) (Jackson Immuno Research Laboratories, 115–035-062; 1:2000).

Drosophila stocks

All fly stocks were maintained at 25°C and 70% relative humidity on a 12-h light/dark cycle and were fed standard yeast-molasses-agar fly food (Fly Media Kitchen, UoFT, contains: Water, yeast, yellow cornmeal, agar, molasses, 10% p-Hydroxy-benzoic acid methyl ester in 95% ethanol). The following fly stocks were used in this study: elavGAL4 (Bloomington, 8765), UAS-park^{RNAi} (Bloomington, 31,259), UAS-mCherry^{RNAi} (Bloomington, 35,785), UAS-LexA^{RNAi} (Bloomington, 67,946). mitoQC flies were generated from the following lines: TH-GAL4 (Bloomington, 8848), CyO: TM6B (Bloomington, 67,157), and UAS-mitoQC flies obtained from Dr. Alex Whitworth (University of Cambridge). Canton (S) and heteroplasmic mtCoI^{T300I} flies were obtained from Dr. Thomas Hurd (University of Toronto).

Drosophila *longevity and climbing assays*

Male Canton-S flies were aged for 7 days on standard fly food before being transferred to vials containing low-melt agarose fly food (2% autoclaved yeast, 7% corn syrup, and a 1.5% mixture of 1:11 standard [Thermo Fisher Scientific Invitrogen, 16,500]:low-melt agarose [BioShop Canada Inc., AGA101.100]) that was supplemented with a combination of either 2.5 mM paraquat, 3.0×10^9 CFU/mL CNCM-I-1079, 1.0×10^{10} CFU/mL R1058, 100 μM MI6C, 5 mM PA, a DMSO vehicle. All fly food that was supplemented with DMSO-solubilized chemicals had a DMSO content below 0.3% to limit toxicological effects [82]. Flies were fed their respective supplemented fly food for 48 h prior to undergoing climbing assays. For heteroplasmic fly experiments, flies were placed in low-melt agarose fly food mixed with the above formulations immediately following eclosion and were incubated at 29°C for 6 days before climbing assays were conducted. In both Canton-S and heteroplasmic fly climbing experiments, 20 flies were transferred to clear plastic cylinder vials and all flies began the climb from the bottom of the vial. Flies were left to climb the vials for 30s and the number of flies that crossed a point 12.5 cm above the cylinder base were counted every 5 s. 6 technical replicates were performed for each group and were averaged to yield a single biological replicate. For survival assays, vials were established with 20 flies each and the number of live flies was counted daily for each vial over 2 weeks. For fly mitoQC experiments, flies expressed a TH driver and mitoQC reporter under the UAS-GAL4 system. Flies were aged for 7 days before being treated with the above probiotics or molecule food formulations. Flies were treated for 7 days before brain dissections were conducted. Fly food vials were changed every 2–3 days for all experiments.

Statistical analysis

The PRKN recruitment screen was analyzed by utilizing a one-way ANOVA to compare baseline PRKN recruitment to probiotic modulated PRKN recruitment at the 100:1 MOI of each strain. PRKN recruitment, phospho-ubiquitin, and mitofusin-2 assays of the top probiotic candidates were analyzed using a one-way ANOVA and Dunnett's multiple comparison post-hoc test to compare the baseline PRKN recruitment/phospho-ubiquitin /mitofusin-2 levels in CCCP-treated cells to those in CCCP-treated cells that were exposed to 10:1, 50:1, and 100:1 probiotic MOIs, probiotic supernatants, and probiotic dead cells. *In vivo* mitoQC assays were analyzed using a mitoQC macro on ImageJ [42] with a smoothing radius of 1.0, ratio threshold of 1.0, and a red channel threshold of 0.5. MitoQC and JC-1 data was analyzed using one-way ANOVAs and Tukey's multiple comparison post-hoc test. Climbing assays were analyzed using a two-way repeated-measures ANOVA to compare all groups at each time point. Longevity analysis was performed using a log-rank (Mantel-Cox) test to compare all treatments. All figure legend sample sizes (n) refer to the number of independent experiments performed and P-values < 0.05 were considered significant.

Acknowledgments

This work was funded from grants to GAM and PJH from MITACS and the CIHR and from MITO2i to JG. Thank you to Olena Gorbenko for technical assistance and for generating the UAS-mitoQC; TH-GAL4 /CyO:TM6B fly line. Thank you to James Jonkman and Judy Cathcart of the AOMF for assistance with confocal imaging experiments. Thank you to Nathalie Simard for assistance with flow cytometry experiments.

Disclosure statement

T.T. is an employee of Rosell Institute for Microbiome and Probiotics, which is the research department of Lallemand Health Solutions. This company researches, manufactures, and distributes probiotic formulations. All other authors declare no competing interests.

Funding

This work was supported by the Mitacs [302553].

Abbreviations

CCCP	carbonyl cyanide m-chlorophenyl hydrazone
CFU	colony-forming units
DMSO	dimethyl sulfoxide
LC3	microtubule associated protein 1 light chain 3
MFN	mitofusin
MI6C	methyl isoquinoline-6-carboxylate
mitoQC	mitochondrial quality control
MOI	multiplicity of infection
mtDNA	mitochondrial DNA
OMM	outer mitochondrial membrane
p-Ub	phosphorylated ubiquitin
PA	picolinic acid
PD	Parkinson disease
PINK1	PTEN induced kinase 1
TH	tyrosine hydroxylase

References

[1] Twelves D, Perkins KS, Counsell C. Systematic review of incidence studies of Parkinson's disease. Mov Disord. 2003;18 (1):19–31.
[2] Tran J, Anastacio H, Bardy C. Genetic predispositions of Parkinson's disease revealed in patient-derived brain cells. NPJ Parkinsons Dis. 2020;6(1):8.
[3] Kitada T, Asakawa S, Hattori N, et al. Mutations in the parkin gene cause autosomal recessive juvenile parkinsonism. Nature. 1998;392(6676):605–608.
[4] Valente EM, Abou-Sleiman PM, Caputo V, et al. Hereditary Early-Onset Parkinson's Disease Caused by Mutations in PINK1. Science. 2004;304(5674):1158–1160.
[5] Bonello F, Hassoun S-M, Mouton-Liger F, et al. LRRK2 impairs PINK1/Parkin-dependent mitophagy via its kinase activity: pathologic insights into Parkinson's disease. Hum Mol Genet. 2019;28 (10):1645–1660.
[6] Bonifati V, Rizzu P, van Baren MJ, et al. Mutations in the DJ-1 Gene Associated with Autosomal Recessive Early-Onset Parkinsonism. Science. 2003;299(5604):256–259.
[7] Funayama M, Ohe K, Amo T, et al. CHCHD2 mutations in autosomal dominant late-onset Parkinson's disease: a genome-wide linkage and sequencing study. Lancet Neurol. 2015;14 (3):274–282.
[8] Lesage S, Drouet V, Majounie E, et al. Loss of VPS13C Function in Autosomal-Recessive Parkinsonism Causes Mitochondrial Dysfunction and Increases PINK1/Parkin-Dependent Mitophagy. Am J Hum Genet. 2016;98(3):500–513.
[9] Ma KY, Fokkens MR, Reggiori F, et al. Parkinson's disease-associated VPS35 mutant reduces mitochondrial membrane potential and impairs PINK1/Parkin-mediated mitophagy. Transl Neurodegener. 2021;10(1):19.
[10] Wilkaniec A, Lenkiewicz AM, Babiec L, et al. Exogenous Alpha-Synuclein Evoked Parkin Downregulation Promotes Mitochondrial Dysfunction in Neuronal Cells. Implications for Parkinson's Disease Pathology. Front Aging Neurosci. 2021;13:591475.
[11] Yamano K, Youle RJ. PINK1 is degraded through the N-end rule pathway. Autophagy. 2013;9(11):1758–1769.
[12] Chan NC, Salazar AM, Pham AH, et al. Broad activation of the ubiquitin-proteasome system by Parkin is critical for mitophagy. Hum Mol Genet. 2011;20(9):1726–1737.
[13] Nguyen TN, Padman BS, Lazarou M. Deciphering the Molecular Signals of PINK1/Parkin Mitophagy. Trends Cell Biol. 2016;26 (10):733–744.
[14] Clark IE, Dodson MW, Jiang C, et al. Drosophila pink1 is required for mitochondrial function and interacts genetically with parkin. Nature. 2006;441(7097):1162–1166.
[15] Park J, Lee SB, Lee S, et al. Mitochondrial dysfunction in Drosophila PINK1 mutants is complemented by parkin. Nature. 2006;441(7097):1157–1161.
[16] Rakovic A, Grünewald A, Kottwitz J, et al. Mutations in PINK1 and Parkin impair ubiquitination of Mitofusins in human fibroblasts. PLoS One. 2011;6(3):e16746.
[17] Truban D, Hou X, Caulfield TR, et al. PINK1, Parkin, and Mitochondrial Quality Control: what can we Learn about Parkinson's Disease Pathobiology? J Parkinsons Dis. 2017;7(1):13–29.
[18] Oliveras-Salva M, Van Rompuy AS, Heeman B, et al. Loss-of-function rodent models for parkin and PINK1. J Parkinsons Dis. 2011;1(3):229–251.
[19] Matheoud D, Cannon T, Voisin A, et al. Intestinal infection triggers Parkinson's disease-like symptoms in Pink1(-/-) mice. Nature. 2019;571(7766):565–569.
[20] Forsyth CB, Shannon KM, Kordower JH, et al. Increased intestinal permeability correlates with sigmoid mucosa alpha-synuclein staining and endotoxin exposure markers in early Parkinson's disease. PLoS One. 2011;6(12):e28032.

[21] Wakabayashi K, Takahashi H, Takeda S, et al. Lewy bodies in the enteric nervous system in Parkinson's disease. Arch Histol Cytol. 1989;52(Suppl):191–194.

[22] Kim S, Kwon SH, Kam TI, et al. Transneuronal Propagation of Pathologic alpha-Synuclein from the Gut to the Brain Models Parkinson's Disease. Neuron. 2019;103(4):627–641.

[23] Aho VTE, Houser MC, Pereira PAB, et al. Relationships of gut microbiota, short-chain fatty acids, inflammation, and the gut barrier in Parkinson's disease. Mol Neurodegener. 2021;16(1):6.

[24] Romano S, Savva GM, Bedarf JR, et al. Meta-analysis of the Parkinson's disease gut microbiome suggests alterations linked to intestinal inflammation. NPJ Parkinsons Dis. 2021;7(1):27.

[25] Tamtaji OR, Taghizadeh M, Daneshvar Kakhaki R, et al. Clinical and metabolic response to probiotic administration in people with Parkinson's disease: a randomized, double-blind, placebo-controlled trial. Clin Nutr. 2019;38(3):1031–1035.

[26] Tan AH, Lim SY, Chong KK, et al. Probiotics for Constipation in Parkinson Disease: a Randomized Placebo-Controlled Study. Neurology. 2021;96(5):e772–e782.

[27] Hsieh TH, Kuo CW, Hsieh KH, et al. Probiotics Alleviate the Progressive Deterioration of Motor Functions in a Mouse Model of Parkinson's Disease. Brain Sci. 2020;**10**(4):206.

[28] Nurrahma BA, Tsao SP, Wu CH, et al. Probiotic Supplementation Facilitates Recovery of 6-OHDA-Induced Motor Deficit via Improving Mitochondrial Function and Energy Metabolism. Front Aging Neurosci. 2021;13:668775.

[29] Moskal N, Riccio V, Bashkurov M, et al. ROCK inhibitors upregulate the neuroprotective Parkin-mediated mitophagy pathway. Nat Commun. 2020;11(1):88.

[30] Gegg ME, Cooper JM, Chau KY, et al. Mitofusin 1 and mitofusin 2 are ubiquitinated in a PINK1/parkin-dependent manner upon induction of mitophagy. Hum Mol Genet. 2010;19(24):4861–4870.

[31] Tanaka A, Cleland MM, Xu S, et al. Proteasome and p97 mediate mitophagy and degradation of mitofusins induced by Parkin. J Cell Biol. 2010;191(7):1367–1380.

[32] Chen Y, Dorn GW 2nd. PINK1-phosphorylated mitofusin 2 is a Parkin receptor for culling damaged mitochondria. Science. 2013;340(6131):471–475.

[33] McLelland GL, Goiran T, Yi W, et al. Mfn2 ubiquitination by PINK1/parkin gates the p97-dependent release of ER from mitochondria to drive mitophagy. Elife. 2018;7. DOI:10.7554/eLife.32866

[34] Gao W, Chen Z, Wang W, et al. E1-like activating enzyme Atg7 is preferentially sequestered into p62 aggregates via its interaction with LC3-I. PLoS One. 2013;8(9):e73229.

[35] Bilen J, Bonini NM. Drosophila as a Model for Human Neurodegenerative Disease. Annu Rev Genet. 2005;39(1):153–171.

[36] Maini Rekdal V, Bess EN, Bisanz JE, et al. Discovery and inhibition of an interspecies gut bacterial pathway for Levodopa metabolism. Science. 2019;364(6445). DOI:10.1126/science.aau6323

[37] Villageliu D, Lyte M Aich P. Dopamine production in Enterococcus faecium: a microbial endocrinology-based mechanism for the selection of probiotics based on neurochemical-producing potential. PLoS One. 2018;13(11):e0207038.

[38] Bingol B, Tea JS, Phu L, et al. The mitochondrial deubiquitinase USP30 opposes parkin-mediated mitophagy. Nature. 2014;510(7505):370–375.

[39] Hosamani R, Muralidhara. Acute exposure of Drosophila melanogaster to paraquat causes oxidative stress and mitochondrial dysfunction. Arch Insect Biochem Physiol. 2013;83(1):25–40.

[40] Wang C, Lu R, Ouyang X, et al. Drosophila overexpressing parkin R275W mutant exhibits dopaminergic neuron degeneration and mitochondrial abnormalities. J Neurosci. 2007;27(32):8563–8570.

[41] Phelps CB, Brand AH. Ectopic gene expression in Drosophila using GAL4 system. Methods. 1998;14(4):367–379.

[42] Lee JJ, Sanchez-Martinez A, Zarate AM, et al. Basal mitophagy is widespread in Drosophila but minimally affected by loss of Pink1 or parkin. J Cell Biol. 2018;217(5):1613–1622.

[43] Montava-Garriga L, Singh F, Ball G, et al. Semi-automated quantitation of mitophagy in cells and tissues. Mech Ageing Dev. 2020;185:111196.

[44] Chen Z, Qi Y, French S, et al. Genetic mosaic analysis of a deleterious mitochondrial DNA mutation in Drosophila reveals novel aspects of mitochondrial regulation and function. Mol Biol Cell. 2015;26(4):674–684.

[45] Coxhead J, Kurzawa-Akanbi M, Hussain R, et al. Somatic mtDNA variation is an important component of Parkinson's disease. Neurobiol Aging. 2016;38(p. 217):e1–217.

[46] de Castro IP, Costa AC, Celardo I, et al. Drosophila ref(2)P is required for the parkin-mediated suppression of mitochondrial dysfunction in pink1 mutants. Cell Death Dis. 2013;4(10):e873.

[47] McNaught KS, Thull U, Carrupt PA, et al. Inhibition of complex I by isoquinoline derivatives structurally related to 1-methyl-4-phenyl-1,2,3,6-tetrahydropyridine (MPTP). Biochem Pharmacol. 1995;50(11):1903–1911.

[48] Sivandzade F, Bhalerao A, Cucullo L. Analysis of the Mitochondrial Membrane Potential Using the Cationic JC-1 Dye as a Sensitive Fluorescent Probe. Biol Protoc. 2019;9(1). DOI:10.21769/BioProtoc.3128

[49] Li Y, Zhu Y, Chu B, et al. Lactobacillus rhamnosus GR-1 Prevents *Escherichia coli*-Induced Apoptosis Through PINK1/Parkin-Mediated Mitophagy in Bovine Mastitis. Front Immunol. 2021;12:715098.

[50] Martin-Maestro P, Gargini R, Perry G, et al. PARK2 enhancement is able to compensate mitophagy alterations found in sporadic Alzheimer's disease. Hum Mol Genet. 2016;25(4):792–806.

[51] Ziviani E, Tao RN, Whitworth AJ. Drosophila parkin requires PINK1 for mitochondrial translocation and ubiquitinates mitofusin. Proc Natl Acad Sci U S A. 2010;107(11):5018–5023.

[52] Hashimoto R, Takahashi S, Hamano K, et al. A new melanin biosynthesis inhibitor, melanoxadin from fungal metabolite by using the larval haemolymph of the silkworm, Bombyx mori. J Antibiot (Tokyo). 1995;48(9):1052–1054.

[53] Takahashi S, Hashimoto R, Hamano K, et al. Melanoxazal, new melanin biosynthesis inhibitor discovered by using the larval haemolymph of the silkworm, Bombyx mori. Production, isolation, structural elucidation, and biological properties. J Antibiot (Tokyo). 1996;49(6):513–518.

[54] Xu Y, Stokes AH, Freeman WM, et al. Tyrosinase mRNA is expressed in human substantia nigra. Brain Res Mol Brain Res. 1997;45(1):159–162.

[55] Carballo-Carbajal I, Laguna A, Romero-Giménez J, et al. Brain tyrosinase overexpression implicates age-dependent neuromelanin production in Parkinson's disease pathogenesis. Nat Commun. 2019;10(1):973.

[56] Fernandez-Pol JA. Morphological changes induced by picolinic acid in cultured mammalian cells. Exp Mol Pathol. 1978;29(3):348–357.

[57] Hara Y, Yanatori I, Tanaka A, et al. Iron loss triggers mitophagy through induction of mitochondrial ferritin. EMBO Rep. 2020;21(11):e50202.

[58] Pan L, Yu J, Mi Z, et al. A Metabolomics Approach Uncovers Differences between Traditional and Commercial Dairy Products in Buryatia (Russian Federation). Molecules. 2018;**23**(4):735.

[59] Zou B, Sun Y, Xu Z, et al. Rapid simultaneous determination of gut microbial phenylalanine, tyrosine, and tryptophan metabolites in rat serum, urine, and faeces using LC-MS/MS and its application to a type 2 diabetes mellitus study. Biomed Chromatogr. 2021;35(2):e4985.

[60] Buňková L, Buňka F, Hlobilová M, et al. Tyramine production of technological important strains of Lactobacillus, Lactococcus and Streptococcus. European Food Res and Tech. 2009;229(3):533–538.

[61] Shao J, Zhu K, Du D, et al. Discovery of 2-substituted-N-(3-(3,4-dihydroisoquinolin-2(1H)-yl)-2-hydroxypropyl)-1,2,3,4-tet rahydroisoquinoline-6-carboxamide as potent and selective protein arginine methyltransferases 5 inhibitors: design, synthesis and biological evaluation. Eur J Med Chem. 2019;164:317–333.

[62] Forkink M, Manjeri GR, Liemburg-Apers DC, et al. Mitochondrial hyperpolarization during chronic complex I inhibition is sustained by low activity of complex II, III, IV and V. Biochim Biophys Acta. 2014;1837(8):1247–1256.
[63] Basit F, van Oppen LM, Schöckel L, et al. Mitochondrial complex I inhibition triggers a mitophagy-dependent ROS increase leading to necroptosis and ferroptosis in melanoma cells. Cell Death Dis. 2017;8(3):e2716.
[64] Yun J, Finkel T. Mitohormesis. Cell Metab. 2014;19(5):757–766.
[65] Baumgart M, Priebe S, Groth M, et al. Longitudinal RNA-Seq Analysis of Vertebrate Aging Identifies Mitochondrial Complex I as a Small-Molecule-Sensitive Modifier of Lifespan. Cell Systems. 2016;2(2):122–132.
[66] Copeland JM, Cho J, Lo T, et al. Extension of Drosophila life span by RNAi of the mitochondrial respiratory chain. Curr Biol. 2009;19(19):1591–1598.
[67] Flones IH, Fernandez-Vizarra E, Lykouri M, et al. Neuronal complex I deficiency occurs throughout the Parkinson's disease brain, but is not associated with neurodegeneration or mitochondrial DNA damage. Acta Neuropathol. 2018;135 (3):409–425.
[68] Rana A, Oliveira MP, Khamoui AV, et al. Promoting Drp1-mediated mitochondrial fission in midlife prolongs healthy lifespan of Drosophila melanogaster. Nat Commun. 2017;8(1):448.
[69] Sprenger HG, Langer T. The Good and the Bad of Mitochondrial Breakups. Trends Cell Biol. 2019;29(11):888–900.
[70] Tian L, Ri H, Qi J, et al. Berberine elevates mitochondrial membrane potential and decreases reactive oxygen species by inhibiting the Rho/ROCK pathway in rats with diabetic encephalopathy. Mol Pain. 2021;17:1744806921996101.
[71] Schneider SM, Girard-Pipau F, Filippi J, et al. Effects of Saccharomyces boulardii on fecal short-chain fatty acids and microflora in patients on long-term total enteral nutrition. World J Gastroenterol. 2005;11(39):6165–6169.
[72] Lee JS, Lee GM. Effect of sodium butyrate on autophagy and apoptosis in Chinese hamster ovary cells. Biotechnol Prog. 2012;28(2):349–357.
[73] Rose S, Bennuri SC, Davis JE, et al. Butyrate enhances mitochondrial function during oxidative stress in cell lines from boys with autism. Transl Psychiatry. 2018;8(1):42.
[74] Bleichner G, Blehaut H, Mentec H, et al. Saccharomyces boulardii prevents diarrhea in critically ill tube-fed patients. A multicenter, randomized, double-blind placebo-controlled trial. Intensive Care Med. 1997;23(5):517–523.
[75] Dalmasso G, Cottrez F, Imbert V, et al. Saccharomyces boulardii inhibits inflammatory bowel disease by trapping T cells in mesenteric lymph nodes. Gastroenterology. 2006;131(6):1812–1825.
[76] Wang C, Li W, Wang H, et al. Saccharomyces boulardii alleviates ulcerative colitis carcinogenesis in mice by reducing TNF-alpha and IL-6 levels and functions and by rebalancing intestinal microbiota. BMC Microbiol. 2019;19(1):246.
[77] Breves G, Faul K, Schröder B, et al. Application of the Colon-Simulation Technique for Studying the Effects of *Saccharomyces boulardii* on Basic Parameters of Porcine Cecal Microbial Metabolism Disturbed by Clindamycin. Digestion. 2000;61(3):193–200.
[78] Buts JP, De Keyser N. Effects of Saccharomyces boulardii on intestinal mucosa. Dig Dis Sci. 2006;51(8):1485–1492.
[79] Luerce TD, Gomes-Santos AC, Rocha CS, et al. Anti-inflammatory effects of *Lactococcus lactis* NCDO 2118 during the remission period of chemically induced colitis. Gut Pathog. 2014;6(1):33.
[80] Mu C, Nikpoor N, Tompkins TA, et al. Probiotics counteract hepatic steatosis caused by ketogenic diet and upregulate AMPK signaling in a model of infantile epilepsy. EBioMedicine. 2022;76:103838.
[81] Seabright AP, Fine NHF, Barlow JP, et al. AMPK activation induces mitophagy and promotes mitochondrial fission while activating TBK1 in a PINK1-Parkin independent manner. FASEB J. 2020;34(5):6284–6301.
[82] Nazir A, Mukhopadhyay I, Saxena DK, et al. Evaluation of the No Observed Adverse Effect Level of Solvent Dimethyl Sulfoxide in Drosophila melanogaster. Toxicol Mech Methods. 2003;13 (2):147–152.